Published in final edited form as:
Neuron. 2011 July 28; 71(2): 306–318. doi:10.1016/j.neuron.2011.05.039.

Spontaneous spiking and synaptic depression underlie noradrenergic control of feed-forward inhibition

Sidney P. Kuo and **Laurence O. Trussell**
Neuroscience Graduate Program and Oregon Hearing Research Center and Vollum Institute, Oregon Health and Science University, Portland, Oregon 97239

Summary

Inhibitory interneurons across diverse brain regions commonly exhibit spontaneous spiking activity, even in the absence of external stimuli. It is not well understood how stimulus-evoked inhibition can be distinguished from background inhibition arising from spontaneous firing. We found that noradrenaline simultaneously reduced spontaneous inhibitory inputs and enhanced evoked inhibitory currents recorded from principal neurons of the mouse dorsal cochlear nucleus (DCN). Together, these effects produced a large increase in signal-to-noise ratio for stimulus-evoked inhibition. Surprisingly, the opposing effects on background and evoked currents could both be attributed to noradrenergic silencing of spontaneous spiking in glycinergic interneurons. During spontaneous firing, glycine release was decreased due to strong short-term depression. Elimination of background spiking relieved inhibitory synapses from depression and thereby enhanced stimulus-evoked inhibition. Our findings illustrate a simple yet powerful neuromodulatory mechanism to shift the balance between background and stimulus-evoked signals.

Introduction

Neurons are rarely silent in the intact brain. Rather, intrinsic and network mechanisms interact to drive action potential firing, even in the absence of external stimuli. For example, multiple classes of inhibitory interneuron exhibit spontaneous spiking behavior *in vivo* (Gentet et al., 2010; Klausberger et al., 2003; Ruigrok et al., 2011) and *in vitro* (Parra et al., 1998). Postsynaptic targets of inhibitory neurons are therefore subject to constantly fluctuating inhibitory synaptic conductances which do not necessarily correspond to stimulus-evoked activity (Alger and Nicoll, 1980; Salin and Prince, 1996; Vincent and Marty, 1996). This background input may impose a tonic inhibition that shapes neuronal integration (Mitchell and Silver, 2003) and can even enhance stimulus encoding if its structure correlates with that of background excitatory inputs (Cafaro and Rieke, 2010). However, numerous studies have also highlighted the importance of stimulus-driven inhibition in controlling the output of target neurons. For example, the precise temporal relationship between afferent-evoked excitation and inhibition imposed by feed-forward inhibitory circuits can strongly regulate spike timing in postsynaptic cells (Mittmann et al., 2005; Pouille and Scanziani, 2001). Despite the prevalence of spontaneous activity in

Corresponding Author: Laurence O. Trussell Oregon Health and Science University 3181 SW Sam Jackson Park Road, L335A Portland, OR 97239 trussell@ohsu.edu.

interneurons, few studies have addressed whether background spontaneous firing affects how stimulus-evoked signals are conveyed by inhibitory cells.

By altering neuronal excitability and/or synaptic transmission, engagement of neuromodulatory systems may provide a general way to adjust the relationship between spontaneous and evoked signals according to environmental and physiological context (Hurley et al., 2004). Noradrenaline (NA) in particular has been implicated in enhancing sensory or stimulus-evoked firing with respect to background activity in several brain regions (Freedman et al., 1976; Hirata et al., 2006; Hurley et al., 2004; Kossl and Vater, 1989; Waterhouse and Woodward, 1980). In the auditory system, the brainstem cochlear nuclei are densely innervated by noradrenergic fibers (Jones and Friedman, 1983; Klepper and Herbert, 1991; Kossl et al., 1988; Kromer and Moore, 1976), but the functional roles of these inputs are not well understood.

Here, we examined how NA affects spontaneous and stimulus-evoked inhibition mediated by cartwheel interneurons of the DCN. Cartwheel cells exhibit variable spontaneous rates (0–30Hz), with average rates typically ~8–13Hz both *in vivo* (Davis and Young, 1997; Portfors and Roberts, 2007) and *in vitro* (Golding and Oertel, 1997; Kim and Trussell, 2007; Manis et al., 1994), and provide strong, glycinergic input to DCN fusiform principal neurons (Mancilla and Manis, 2009; Roberts and Trussell, 2010). Within the molecular layer of the DCN, parallel fiber axons originating from DCN granule cells convey excitatory input from multiple sensory modalities to cartwheel cells as well as to fusiform cells (Oertel and Young, 2004). This shared input between cartwheel and principal cells forms the basis for a feed-forward inhibitory network (Roberts and Trussell, 2010) that powerfully filters the acoustic responses of principal neurons (Davis et al., 1996; Davis and Young, 1997; Shore, 2005).

We found that NA enhanced inhibition elicited by parallel fiber stimulation while simultaneously reducing spontaneous inhibitory input to fusiform cells. This dual effect resulted in a large increase in the signal-to-noise ratio of parallel fiber-evoked feed-forward inhibition. Remarkably, the opposing effects of NA upon spontaneous and evoked inhibition were both due to noradrenergic elimination of cartwheel cell spontaneous spiking. Under control conditions, cartwheel synapses were tonically depressed by background spiking activity. By shutting off spontaneous spiking, NA relieved cartwheel synapses from depression and thereby enhanced glycine release in response to parallel fiber stimulation. This novel mechanism for neuromodulation, in which synaptic output is indirectly controlled through modulation of spontaneous activity, may have distinct advantages over direct regulation of presynaptic release probability in spontaneously firing cells.

Results

Noradrenaline enhances feed-forward inhibition

We examined whether NA affects integration of excitatory and inhibitory signals conveyed through the molecular layer circuitry of the DCN. Whole-cell voltage-clamp recordings were acquired from fusiform cells in acute slices of mouse brainstem and synaptic currents were recorded in response to activation of parallel fibers by an extracellular stimulating electrode positioned in the DCN molecular layer (Figure 1A). Single stimuli typically elicited weak excitatory currents and small or undetectable inhibitory currents (see first stimulus, Figure 1B, top). Because parallel fibers exhibit strong short-term facilitation (Roberts and Trussell, 2010; Tzounopoulos et al., 2004), brief stimulus trains (three stimuli at 20 Hz) were applied to recruit robust parallel fiber activity. When fusiform cells were clamped at −60 mV, intermediate to the reversal potentials for Cl^- conductances (−84 mV) and excitatory conductances (~0 mV), each stimulus elicited a sequence of inward current

followed closely by outward current (Figure 1B), characteristic of direct activation of excitatory fibers followed by feed-forward recruitment of inhibitory inputs (Mittmann et al., 2005; Pouille and Scanziani, 2001). Both inward and outward components of the responses were larger for the second and third parallel fiber stimuli due to facilitation of excitatory inputs onto both fusiform and cartwheel cells (Roberts and Trussell, 2010). Consistent with activation of disynaptic inhibition, inward and outward components of the evoked responses were largely abolished by application of NBQX (Figure 1C).

When identical stimulus trains were applied in the presence of 10 μM NA, we observed a significant enhancement of the outward components of evoked currents in response to the second and third stimuli (Figure 1B, middle, D; measured as total outward charge, see Methods; stim2 control: 701±246 pA*ms, NA: 1809±561 pA*ms, $p<0.05$, n= 6; stim3 control: 596±203 pA*ms, NA: 1680±286 pA*ms; $p<0.01$, n=6). This effect could be clearly visualized by subtracting average control responses from average currents recorded in NA (Figure 1B, bottom). Quantification of total charge in such subtracted records demonstrated a large net increase in the charge following the second and third stimuli (Figure 1E; stim2 1158±421 pA*ms; stim 3 1271±261 pA*ms, $p<0.05$ and <0.005, respectively, one sample t-test comparison to 0 pA*ms). On average a small reduction in the total charge was observed following the first stimulus (Figure 1E; −216±47 pA*ms, $p<0.05$, one sample t-test comparison to 0 pA*ms).

The enhancement of net outward synaptic current by NA could reflect an increase in inhibitory conductance and/or a decrease in excitatory conductance. NA did not have any effect on the peak amplitude (EPSC1 control: −203±39 pA, NA: −195±31 pA, p=0.40, n=5) or short-term facilitation (EPSC2/1 control: 1.73± 0.27, NA: 1.69±0.28; p=0.59; EPSC3/1 control 1.92±0.77, NA: 1.93±0.38, p=0.93, n=5) of evoked parallel fiber EPSCs recorded from fusiform cells (inhibitory transmission blocked with 10 μM gabazine, 0.5 μM strychnine) (Figure S1). Thus, NA specifically altered inhibitory input to fusiform cells.

NA increases signal-to-noise ratio of feed-forward inhibition

In addition to the enhancement of stimulus-evoked inhibitory postsynaptic currents (IPSCs), we also observed that NA sharply reduced spontaneous IPSCs (sIPSCs) recorded in fusiform cells (Figure 2A). Application of NA (10 μM) significantly decreased both frequency (Figure 2B; mean frequency control: 93.0±8.2 Hz, NA: 15.3±3.9 Hz; $p<0.001$, paired t-test, n=6) and peak amplitude (Figure 2C; control 78.9±6.5 pA, NA 46.6±4.3 pA; $p<0.01$, paired t-test, n=6) of spontaneous events in all cells tested.

The opposing effects of NA upon spontaneous and parallel fiber stimulation-evoked IPSCs led to a dramatic shift in the balance between these two modes of inhibitory input. In control, sIPSCs occurred frequently and often had amplitudes similar to those evoked by parallel fiber stimulation (Figure 3A, top). In the presence of NA, the near elimination of spontaneous IPSCs together with the enhancement of stimulus-evoked IPSCs resulted in a marked difference between stimulus-driven versus background currents (Figure 3A, bottom). To quantify the change in background input produced by NA, we measured root-mean-square (RMS) values of individual current sweeps over a 250 ms period just prior to parallel fiber stimulation (left side of Figure 3A). NA (10 μM) significantly reduced the RMS of background currents (Figure 3B; control: 33.06±4.45 pA, NA: 13.79±1.23 pA, $p<0.005$, n=6). We quantified the change in relative amplitudes between evoked and spontaneous currents by dividing evoked IPSC peak amplitudes by the RMS of background currents (signal-to-noise ratio). Signal-to-noise of the first parallel fiber stimulus was not significantly changed between control and NA (1.36±0.50 and 2.83±1.36, respectively; p=0.16), but NA application resulted in a 7–8-fold change in signal-to-noise ratios for the second and third stimuli in a train (stim2 control: 3.3±1.3, NA: 23.2±6.9, $p<0.02$; stim 3

control 2.8±0.7, NA: 22.1±3.9, $p < 0.005$; n=6; Figure 3C). These results indicate that in the presence of NA, feed-forward inhibition evoked by parallel-fiber activity dominates over spontaneous inputs.

Activation of α_2 adrenergic receptors eliminates cartwheel cell spontaneous spiking

DCN principal neurons receive inhibitory inputs from several subtypes of interneuron (Oertel and Young, 2004). However, the noradrenergic elimination of fusiform cell sIPSCs is probably due to effects of NA on the spontaneous firing of presynaptic cartwheel cells. First, cartwheels are the most numerous molecular layer interneuron type (Lorente de No, 1981) and have a high probability of forming strong synaptic connections onto nearby fusiform cells (Mancilla and Manis, 2009; Roberts and Trussell, 2010). Second, >75% of cartwheel cells fire spontaneously under similar recording conditions to those used here (Kim and Trussell, 2007). Finally, cartwheel cells are distinguished from other DCN neurons by their ability to fire high-frequency (~200 Hz) bursts of action potentials termed complex spikes (Kim and Trussell, 2007; Manis et al., 1994; Zhang and Oertel, 1993) and complex spike-like bursts of spontaneous IPSCs were frequently observed in all cells (Golding and Oertel, 1997; Roberts and Trussell, 2010).

We therefore investigated whether NA affects cartwheel cell spontaneous behavior using extracellular loose cell-attached recordings. Consistent with previous results (Kim and Trussell, 2007), 72.4% (63/87 cells) of cartwheel cells fired APs spontaneously in control conditions. Also in agreement with previous work (Golding and Oertel, 1997; Kim and Trussell, 2007), control spontaneous spiking was not regular but instead was characterized by brief periods of spiking activity separated by periods of quiescence, each of which could last from ~0.5 s up to several seconds (Figure 4A). Spiking periods consisted primarily of simple spikes occurring at a frequency of ~20–30 Hz (Figure 4B–C) and in 6/11 cells included one or two high-frequency (~200 Hz) complex spike bursts per spiking period ("complex spiking" Figure 4B–C). The mean firing rate in control was 13.6±2.0 Hz (range 4.5 to 25.9 Hz, n= 11).

NA application (10 μM) resulted in almost complete elimination of spontaneous spiking in all cartwheel cells tested (Figure 4A–B, D–F; spike rate reduced to 4.8±3.0% of control, n= 6). This effect was reversed by the α_2-adrenergic receptor antagonist idazoxan (1 μM; Figure 4E–F; 101.9±7.3% control spike rate in NA + idazoxan, n= 5; not significantly different than 100 % control rate, p=0.80, one-sample t-test) and was mimicked by the α_2 agonists UK14304 (1 μM; 19.8±10.4% control rate, n= 8) and clonidine (5 μM; 14.8±13.0% control rate, n=4) (Figure 4F). In contrast, NA was equally effective at eliminating cartwheel spiking when applied alone, or in the presence of the α_1 antagonist prazosin (0.1 μM) or the β receptor antagonist propranolol (20 μM) (Figure 4F; NA reduced spike rate to 8.2±7.3%, n=4, and 0.8±0.8%, n=6, of control, respectively). Thus, NA silences cartwheel cell spontaneous spiking and this effect is mediated solely by α_2 adrenergic receptors.

NA does not directly affect synaptic transmission

NA could affect parallel fiber-evoked inhibition of fusiform cells through several potential mechanisms. NA is known to directly alter neurotransmitter release from multiple cell types by activating adrenergic receptors located on or near presynaptic axon terminals (Kondo and Marty, 1997; Leao and Von Gersdorff, 2002). We therefore examined whether direct enhancement of glutamate release from parallel fibers onto cartwheel cells and/or glycine release from cartwheel cell terminals could account for the observed increase in parallel fiber-evoked feed-forward inhibition of fusiform cells induced by NA.

To determine whether noradrenergic strengthening of parallel fiber inputs could contribute to enhanced recruitment of cartwheel cell activity, we made whole-cell recordings from cartwheel cells and measured EPSCs in response to parallel fiber stimulation (inhibitory currents blocked with 10 μM gabazine, 0.5 μM strychnine)(Figure 5A–B). NA did not alter the peak amplitude (Figure 5C; EPSC1 in control: −382±105 pA, NA: −336±85 pA, p=0.30, n=6) or short-term facilitation (Figure 5D; EPSC2/EPSC1 control: 2.25±0.12, NA: 2.14±0.11, p=0.39, n=6; EPSC3/EPSC1 control: 2.96±0.23, NA: 2.75±0.14, p=0.19, n=6) of parallel fiber EPSCs. Thus, the increase in feed-forward inhibition of fusiform cells was not due to a change in excitatory input to cartwheel cells. To test whether NA could act directly on cartwheel cell axon terminals to modulate glycine release, we acquired simultaneous whole-cell recordings from synaptically connected pairs of cartwheel and fusiform cells. Three simple spikes at 20-ms intervals were elicited by brief depolarizing current injections into presynaptic cartwheel cells held in current clamp and the resulting unitary IPSCs (uIPSCs) were recorded in postsynaptic fusiform cells held in voltage clamp (Figure 5E). NA application did not alter the peak amplitude (Figure 5F; uIPSC1 in control: 557±176 pA, NA: 552±187 pA, p=0.89, n=6 pairs) or short-term depression (Figure 5G; uIPSC2/uIPSC1 control: 0.55±0.02, NA: 0.59±0.01, p=0.10, n=6 pairs; uIPSC3/uIPSC1 control: 0.40±0.01, NA: 0.42±0.01, p=0.31, n=6 pairs) of uIPSCs. Thus, NA does not change spontaneous or evoked cartwheel cell-mediated inhibition of fusiform neurons by directly affecting release from cartwheel synapses. Taken together with the lack of effect on EPSCs, it appears that NA regulates inhibitory transmission through a mechanism completely independent of conventional presynaptic modulation.

Subthreshold changes in somatic membrane potential (V_m) can alter synaptic transmission (Alle and Geiger, 2006; Shu et al., 2006). Because NA likely exerted its effects on spontaneous spiking by hyperpolarizing cartwheel cells, we examined cartwheel synaptic output in three additional connected cartwheel and fusiform cell pairs while holding the presynaptic cartwheel V_m at either −79.4±0.9 mV (V_{rest}) or −89.6±0.6 mV ($V_{hyperpol}$) using bias current injection in current-clamp (not shown). Both potentials were below threshold for spontaneous firing. Hyperpolarization of V_m did not affect uIPSC peak amplitude (uIPSC1 V_{rest} 834±346 pA, $V_{hyperpol}$ 802±332, p=0.39; uIPSC1 $V_{hyperpol}/V_{rest}$ 0.97±0.02) or short-term depression in response to trains of presynaptic action potentials (3 APs at 50 Hz) (uIPSC2/1 V_{rest} 0.57±0.02, $V_{hyperpol}$ 0.53±0.03, p=0.35; uIPSC3/1 V_{rest} 0.43±0.06, $V_{hyperpol}$ 0.44±0.03, p=0.79).

Noradrenergic enhancement of feed-forward inhibition requires α_2-adrenergic receptors

We wondered whether elimination of spontaneous cartwheel spiking might somehow contribute to the enhancement of feed-forward inhibition by NA. Because silencing of cartwheel cell spontaneous spiking was dependent on α_2-adrenergic receptors (Figure 4E–F), we tested whether α_2-receptors were similarly required for the noradrenergic enhancement of feed-forward inhibition. Current responses to parallel fiber train stimulation were recorded in fusiform cells in control conditions, then in NA (10 μM), followed by NA (10 μM) and idazoxan (1 μM) (Figure 6A). NA again strongly enhanced outward currents evoked by the second and third stimuli (Figure 6B; outward charge stim 2 control: 1425±397 pA*ms, NA: 3618±609 pA*ms, p<0.001, n=5; stim 3 control: 1158 pA*ms, NA: 4065±946 pA*ms, p<0.01, n=5). Idazoxan reduced the NA-induced enhancement of outward charge in all cells tested, resulting in a complete reversal of the NA effect on feed-forward inhibition for the second stimuli (outward charge in NA + idazoxan: 1953±526 pA*ms, comparison to control: p=0.097, n=5) and near complete reversal for the third stimulus (Figure 6B; 1665±419 pA*ms, comparison to control: p=0.047, n=5). When averaged currents recorded during the baseline control period were subtracted from those recorded during co-application of NA and idazoxan, only a minor increase in the total

current was revealed for each of the stimuli (Figure 6C–D; stim1: 193±159 pA*ms; stim 2: 610±225 pA*ms; stim 3: 572±175 pA*ms). This was in contrast to the large total charge difference following the second and third stimuli measured from currents obtained from subtraction of control traces from those obtained during NA application (Figure 6C–D; stim 1: 200±247 pA*ms; stim 2: 2279±263 pA*ms; stim 3: 2950±635 pA*ms). Thus, α_2-receptors were the primary adrenergic receptor subtype mediating the noradrenergic enhancement of feed-forward inhibition.

Spontaneous spiking depresses cartwheel cell synaptic transmission

The shared dependence on α_2 adrenergic receptors of noradrenergic modulation of cartwheel cell spontaneous firing (Figure 4) and feed-forward inhibition of fusiform cells (Figure 6) suggested a potential link between the two effects. Taking into account that our initial examination of cartwheel synapses onto fusiform cells demonstrated strong short-term depression at this synapse (Figure 5), we hypothesized the constant background spontaneous firing of cartwheel cells in control conditions would lead to persistently depressed cartwheel synaptic output. As a result of tonic synaptic depression, cartwheel-mediated IPSCs onto fusiform cells evoked by parallel fiber stimulation would be weakened in control conditions. However, the loss of spontaneous spiking in the presence of NA should permit cartwheel synapses to recover from depression and thus result in robust stimulus-evoked inputs to fusiform neurons.

As an initial examination of this hypothesis, we characterized synaptic depression at cartwheel synapses using simultaneous whole-cell recordings from connected pairs of cartwheel and fusiform neurons. Current injection was used to trigger an initial simple spike or complex spike burst (3–4 spikelets) in presynaptic cartwheel cells, which was then followed by a second simple spike at intervals between 50 ms to 15 seconds after the first simple/complex spike. The resulting uIPSCs were recorded in postsynaptic fusiform cells (example responses to initial presynaptic simple spike, Figure 7B; initial presynaptic complex spike, Figure 7C). These experiments revealed strong synaptic depression at short test intervals (intervals from 50–500 ms, depressed by 35.1±1.0% (initial simple spike) or by 69.4±0.8% (initial complex spike) of first uIPSC peak amplitude). The time courses of recovery from depression were well fitted by exponential functions with similar time constants for recovery (5.8±0.9 seconds and 5.5±0.9 seconds following an initial simple or complex spike, respectively; Figure 7D).

The relatively slow time course of recovery from depression at cartwheel to fusiform cell synapses indicated these synapses would likely be depressed during control conditions, since spontaneously active cartwheels typically exhibited spiking with mean interspike intervals <1 second (Figure 4C). To directly confirm that spontaneous spiking resulted in depression, additional recordings from connected cartwheel and fusiform pairs were performed in which constant bias current injection was used to induce presynaptic cartwheel cells to fire at various background rates (Figure 7E–F). These experiments demonstrated a clear relationship between presynaptic firing rate and postsynaptic uIPSC amplitude (mean spike rate range 0.7 to 13.8 Hz; uIPSC depressed from 38.0% to 89.9% of peak amplitude without background firing; Figure 7F). Thus, cartwheel synapses were persistently depressed at the background firing rates observed under control conditions.

Modulation of spontaneous firing in a single presynaptic interneuron reproduces NA effect on feed-forward inhibition

If noradrenergic control of cartwheel background spiking accounts for the NA-induced changes in parallel fiber-evoked feed-forward inhibition then modulating cartwheel spontaneous spiking independent of NA should also alter feed-forward inhibition. To test

this, simultaneous recordings were acquired from connected cartwheel-fusiform pairs while parallel fibers onto both cells were stimulated (Figure 8A). This configuration allowed us to control the firing rate of a presynaptic cartwheel using constant bias current injection while assessing any potential changes in the fusiform cell response to parallel fiber stimulation. In each experiment, stimulus position and strength was adjusted to elicit both stimulus-evoked spiking in the presynaptic cartwheel cell and feed-forward inhibition in the post-synaptic fusiform neuron.

Parallel fiber stimulus-evoked spiking in the presynaptic cartwheel was slightly changed in the absence of background spiking, with a lower probability of spiking on the first stimulus compared to the background spiking condition (compare Figure 8B, middle traces). Complex spikes were also sometimes more readily elicited by stimuli applied on a background of spontaneous firing. This can be attributed to differences in cartwheel excitability at the different levels of bias current injection.

More importantly, the outward component of the postsynaptic fusiform responses to the second stimulus in the train was significantly enhanced when the presynaptic cartwheel did not spike spontaneously in all cartwheel-fusiform pairs tested (compare bottom traces in Figure 8B; summary for 1.4 to 6.6 Hz background presynaptic firing rates in Figure 8C; stim 2 mean outward charge with background firing: 1388±208 pA*ms, no background firing: 2520±366 pA*ms, $p<0.05$, n=4 pairs). Total charge measurements from traces created by subtracting averaged fusiform currents obtained during background spiking in patch-clamped presynaptic cartwheels from those recorded without presynaptic background firing (see example Figure 8D) demonstrated a clear enhancement of outward charge following the second stimulus (Figure 8E; stim 2 1173±357 pA*ms).

Thus, changing cartwheel spontaneous spiking activity by intracellular current injection alone was sufficient to alter parallel fiber-evoked feed-forward inhibition. In fact, the change in outward current following the second stimulus was remarkably similar to that observed previously in response to NA (compare Figures 1F, 6D, 8B). These results support the idea that NA enhances feed-forward inhibition by indirectly relieving cartwheel synapses from depression through elimination of spontaneous action potential firing in a small number of connected presynaptic cartwheel cells.

In contrast to the effects of NA, the response to the third stimulus was unchanged between the presynaptic background spiking versus no spiking conditions (Figure 8B; outward charge with background firing: 1149±494 pA*ms, no background firing: 1317±434 pA*ms, $p=0.14$, n=4 pairs). However, this likely reflected limitations of our experimental approach. In the paired recording experiments shown in Figure 8, parallel fiber stimuli were adjusted to evoke presynaptic cartwheel spikes reliably by the second stimulus in the train under both background spiking and no background spiking conditions. Thus, synapses from the presynaptically recorded cartwheel cell were usually strongly depressed by the third stimulus in either condition, and therefore likely contributed a similar amount to the total current following the third stimulus both with and without background spiking. With NA application (Figures 1, 6), spontaneous rate in all presynaptic cartwheel cells, rather than a single neuron, should have been affected. The change in inhibitory input for both the second and third stimuli with NA was probably due to recruitment of multiple cartwheel cells with varying levels of stimulus-evoked parallel fiber input and/or spike thresholds.

Discussion

For diverse inhibitory cell types, stimulus-evoked action potential output occurs against a background of spontaneous spiking activity. Although background inhibitory inputs can

contribute to information processing (Cafaro and Rieke, 2010; Mitchell and Silver, 2003), the presence of background activity raises the issue of whether stimulus-driven signals can be differentiated from those driven by spontaneous activity in postsynaptic targets.

We identified a neuromodulatory mechanism that robustly alters the balance between spontaneous and evoked inhibitory signals received by DCN principal neurons. By simultaneously reducing spontaneous inhibitory currents while increasing afferent-evoked inhibition, NA shifted the mode of inhibition of fusiform cells strongly in favor of inhibition driven by parallel fiber activity. This mechanism is distinct from other possible strategies for differentiating between evoked and background activity. These include coordinating stimulus-evoked activity among a population of presynaptic neurons (Swadlow, 2002), encoding stimuli as changes in firing frequency in relation to background rates (Telgkamp and Raman, 2002), and presynaptic inhibition (Frerking and Ohliger-Frerking, 2006). These mechanisms could also potentially contribute to enhancement of signal-to-noise at the cartwheel to fusiform synapse, but their effectiveness might be limited for several reasons. First, cartwheel cells do not commonly share single excitatory input fibers, and even a single cartwheel cell can strongly inhibit postsynaptic fusiform neurons (Roberts and Trussell, 2010). Thus, activation of multiple cartwheel cells, which would depend on specific patterns activity in the granule cell population, is not necessary to affect fusiform output. Second, cartwheel cells spontaneous firing is not regular, but instead occurs in bursts, thus complicating firing rate-based representations of stimuli. Moreover, the temporal relationship between excitatory and inhibitory signals arising from parallel fiber activity might not be preserved if stimuli were simply encoded as a change in cartwheel cell firing rate. Finally, at hippocampal synapses presynaptic inhibition is proposed to function as a high-pass filter to differentiate high-frequency signals evoked by sensory stimuli from lower frequency background activity (Frerking and Ohliger-Frerking, 2006), but cartwheel cell spontaneous firing often includes high-frequency bursts of activity (i.e. complex spikes).

Indirect versus direct modulation of synaptic transmission

Presynaptic nerve terminals are common targets of neuromodulators . However, we found that the dual effects of NA upon spontaneous and evoked activity were both mediated by noradrenergic silencing of cartwheel cell spontaneous spiking, rather than a direct effect upon presynaptic release probability. By targeting cartwheel cell spontaneous spiking, NA not only reduced spontaneous IPSCs in fusiform cells, but also indirectly strengthened stimulus-evoked cartwheel cell-mediated IPSCs by relieving cartwheel synapses from a chronically depressed state. If instead, NA had acted directly upon cartwheel terminals to enhance release probability independent of spontaneous firing, the result would likely be an enhancement of both spontaneous and stimulus-evoked output. By coordinating the strength of stimulus-evoked output with background firing rate, selective targeting of spontaneous spiking produced an enhancement of signal-to-noise ratio that would not likely be achieved by direct enhancement of release probability.

It is also informative to contrast our observations with less selective actions of neuromodulators in other brain regions. For instance, depolarization-induced release of endogenous cannabinoids from Purkinje cells suppresses both spontaneous firing and presynaptic release probability of molecular layer interneurons in the cerebellum (Kreitzer et al., 2002). Although background inhibitory input to Purkinje cell is reduced by these dual actions of endocannabinoids, evoked responses are similarly reduced due to the decrease in presynaptic release probability (Kreitzer et al., 2002).

Synaptic depression and spontaneous spiking

Our results are consistent with and extend previous studies demonstrating an important relationship between short-term synaptic depression and background firing rate. *In vitro* slice recordings have revealed suppression of postsynaptic currents by *in vivo* spontaneous activity patterns at the calyx of Held synapse (Hermann et al., 2007) and giant corticothalamic synapses between somatosensory cortex and thalamus (Groh et al., 2008). *In vivo* studies have observed that spontaneous activity of thalamic neurons results in tonic depression of thalamocortical synapses in primary somatosensory (Castro-Alamancos and Oldford, 2002) and visual cortices (Boudreau and Ferster, 2005). Thus, depression of synaptic output by spontaneous patterns of spiking activity appears to be a common phenomenon. Our experiments show that selective control of background spike rate provides a powerful way to alter synaptic output at synapses that exhibit short-term depression. Neuromodulatory control of spontaneous firing may therefore represent a general mechanism to shift between distinct modes of signaling according to behavioral context (Castro-Alamancos and Oldford, 2002).

Inhibition of spontaneous firing by activation of α_2 adrenergic receptors

The elimination of spontaneous firing in cartwheel cells by activation of α_2 adrenergic receptors is consistent with the effects of α_2 receptors on other spontaneously active neurons (Hirono and Obata, 2006; Li and van den Pol, 2005; Solis and Perkel, 2006; Williams and North, 1985). α_2 adrenergic receptors generally mediate inhibitory actions of NA. A primary consequence of α_2 receptor activation in many cell types is the opening of G-protein-activated inwardly rectifying potassium channels (GIRKs) (Williams et al., 1985). Other effects include inhibition of voltage-gated calcium channels (Bean, 1989; Dunlap and Fischbach, 1981) and reductions in cyclic nucleotide gated (HCN) channel activity (Carr et al., 2007). The specific mechanism(s) underlying loss of spontaneous cartwheel cell firing were not examined in the present study, but previous studies have generally shown that depression of spontaneous activity by α_2 receptors is primarily a result of hyperpolarization due to GIRK channel activation (Arima et al., 1998; Li and van den Pol, 2005; Williams et al., 1985; Williams and North, 1985). We therefore consider it likely that activation of GIRK channels underlies the loss of spontaneous spiking in cartwheel cells.

Implications for auditory processing

This study adds to growing evidence that the DCN molecular layer circuitry is subject to modifications by specific patterns of afferent activity (Fujino and Oertel, 2003; Tzounopoulos et al., 2004; Tzounopoulos et al., 2007) as well as extrinsic and intrinsic neuromodulatory systems (Bender et al., 2010; Zhao et al., 2009; Zhao and Tzounopoulos, 2011). Although the specific role of the molecular layer circuitry in auditory processing is not fully understood, the ability to flexibly adapt molecular layer output according to previous activity or physiological context may contribute importantly to DCN function (Oertel and Young, 2004). One prominent hypothesis regarding DCN function is that proprioceptive information conveyed by parallel fibers is integrated with spectral information from auditory inputs to contribute to sound localization (May, 2000; Oertel and Young, 2004; Sutherland et al., 1998). An additional proposal is that, by analogy to cerebellum-like electrosensory structures in weakly electric fish, the DCN molecular layer circuitry functions as an adaptive filter to cancel sounds that are not behaviorally relevant, such as self- or movement-generated noise (Bell et al., 2008; Oertel and Young, 2004). Importantly, both proposed functions rely upon the ability of activity in parallel fibers to recruit robust inhibition of principal neurons. By strongly enhancing parallel fiber stimulus-evoked inhibition, the actions of NA may contribute critically to the filtering of auditory signals by the cartwheel cell network. It will therefore be important to determine under what conditions NA is released in the DCN. Similar to other brain regions, noradrenergic

innervation of DCN appears to arise primarily from locus coeruleus (LC) (Klepper and Herbert, 1991; Thompson, 2003). LC neurons exhibit tonic spiking activity that is highest during awake states and absent during REM sleep. Additionally, firing in these neurons can be briefly elevated above tonic levels ("phasic" responses) when an animal attends to behaviorally relevant stimuli (Berridge and Waterhouse, 2003). How these activity patterns correspond to release of NA in the DCN remains to be investigated, but a reasonable assumption is that NA levels are elevated during vigilant states corresponding to high levels of LC activity. Thus, noradrenergic modulation of cartwheel cell output may permit selective filtering of auditory information during awake and attentive states.

Materials and Methods

Slice preparation

All procedures used in the care and handling of animals were approved by the OHSU Institutional Animal Care and Use Committee. Parasagittal brainstem slices (210 μm) were prepared from postnatal day 17–23 heterozygous transgenic GIN (**G**FP-expressing **I**nhibitory **N**eurons) (Oliva et al., 2000) or GlyT2-GFP mice (Zeilhofer et al., 2005) and their wild-type littermates. Both transgenic lines were backcrossed into the C57BL/6J genetic background (Jackson Labs) and were maintained and genotyped as previously described (Roberts et al., 2008). No differences were observed across genotypes so data from all mouse strains were pooled. Slices were prepared then maintained for 1 hour in warm (~34°C) ACSF solution containing (in mM): 130 NaCl, 2.1 KCl, 1.7 $CaCl_2$, 1.0 $MgSO_4$, 1.2 KH_2PO_4, 20 $NaHCO_3$, 3 Na-HEPES, 11 glucose; bubbled with 5% CO_2/ 95% O_2, ~300 mOsm. Slices not transferred to the recording chamber immediately following the one-hour recovery period were maintained in the same solution at room temperature (~22°C) until use.

Electrophysiology

During recordings, slices were constantly perfused (~1–2 mL/min) with ACSF maintained at 33 ± 1°C. Cells were visualized on the stage of an upright microscope (Olympus BX51W) using infrared gradient contrast optics (Dodt et al., 2002) and a 60X magnification objective. Fusiform cells and cartwheel cells were identified based on location within the slice, somatic size and morphology, and characteristic responses to hyperpolarizing and depolarizing current injections (Golding and Oertel, 1997; Manis et al., 1994; Tzounopoulos et al., 2004; Zhang and Oertel, 1994). In loose cell-attached recordings, spontaneously active cartwheel cells could be easily identified by their irregular action potential firing patterns (Kim and Trussell, 2007). Additionally, EGFP expression in tissue from GIN (subset of GAD67-expressing cells labeled) or GlyT2-EGFP (all glycinergic neurons labeled) transgenic mice was often used to facilitate cell identification (Roberts and Trussell, 2008). For whole cell recordings, electrodes were filled with a solution containing (in mM): 113 K-Gluconate, 9 HEPES, 2.75 $MgCl_2$, 1.75 $MgSO_4$, 0.1 EGTA, 14 $Tris_2$-phosphocreatine, 4 Na_2-ATP, 0.3 Tris-GTP; osmolality adjusted to ~290 mOsm with sucrose, pH adjusted to 7.25 with KOH. All reported membrane potential values are corrected for a −10 mV junction potential. For loose cell-attached recordings, pipettes were filled with a modified ACSF solution containing (in mM): 142 NaCl, 2.1 KCl, 1.7 $CaCl_2$, 1.0 $MgSO_4$, 1.2 KH_2PO_4, 10 Na-HEPES, 11 glucose; ~300 mOsm, pH adjusted to 7.35 with NaOH. Patch pipettes (2–4 MΩ) were pulled from borosilicate glass (WPI). For loose cell-attached experiments, 10 μM NBQX, 50 μM D-APV, 0.5 μM strychnine, 10 μM SR95531 (gabazine) were added to all bath solutions to block excitatory and inhibitory synaptic transmission. Bath solutions for whole cell recordings did not contain drugs unless specified otherwise. To stimulate parallel fibers, voltage pulses (10–30 V, 150–200 μsec) were applied via ACSF-filled double-barreled glass electrodes (lengthwise tip diameter ~5 μm; theta glass, WPI) that were

positioned in the molecular layer >~100 μm from the soma of recorded cells. Paired recordings targeted nearby neurons (<50 μm intersomatic distance). In close agreement with previous results (Roberts and Trussell, 2010), we found functional cartwheel to fusiform cell synaptic connections in 35 out of 98 tested cartwheel-fusiform pairs (35.7 % connection probability).

Data acquisition and analysis

Recordings were acquired using a Multiclamp 700B amplifier and pClamp 10 software (Molecular Devices). Signals were digitized at 10–50 kHz using a Digidata 1322A (Molecular Devices) and low-pass filtered at 3–10 kHz. For all voltage-clamp experiments, series resistance (<20 MΩ) was compensated by 80% and membrane potential was held constant at −60 mV. To quantify changes in stimulus-evoked currents (Figures 1D, 6D, 8B), total outward charge was measured from averaged current traces (Figures 1, 6: 20 sweeps in each experimental condition; Figure 8, 13 to 33 sweeps per condition) by integrating all current within a window that started at the first zero current level crossing following stimulus onset and ending 20 ms after stimulus onset. Charge difference (Figure 1F, 6F, 8E) was measured from subtracted currents (see Figures 1E, 6E, 8D) over 20 ms windows that started 1 ms after stimulus onset. Spontaneous IPSCs occurring within 250 ms windows prior to parallel fiber stimulus application (15 sec inter-sweep interval) were detected using the template function event detection feature in Axograph X. Root mean square (RMS) measurements for spontaneous currents were determined from current amplitude values for every point (50 kHz acquisition, 10 kHz filtering) within the same time windows used to detect sIPSCs. All data are reported as mean ± SEM. Unless otherwise stated, statistical significance ($p<0.05$) was tested using paired or unpaired Student s t-tests as appropriate.

Reagents

NBQX, D-APV, strychnine and gabazine were obtained from Ascent Scientific. All other drugs and chemicals were from Sigma Aldrich. Stocks of NA were prepared fresh from (+/−)-Noradrenaline (+)-bitartate powder each day. Bath solutions containing NA were protected from light to minimize oxidation. Final concentration of NA was 10 μM in all experiments except those in Figure S1 (50 μM NA). All drugs were applied via bath perfusion.

Supplementary Material

Refer to Web version on PubMed Central for supplementary material.

Acknowledgments

We are grateful to Pierre Apostolides and Drs. Hai Huang, Haining Zhong and Craig Jahr for helpful discussions and to Elizabeth Brodeen-Kuo and Drs. Kevin Bender and John Williams for advice and suggestions on the manuscript. We thank Dr. Sascha du Lac for providing GIN and GlyT2-EGFP mice. This work was supported by NIH grants RO1DC004450 (L. O. T.) and F31DC010120 (S. P. K.).

References

Alger BE, Nicoll RA. Spontaneous inhibitory post-synaptic potentials in hippocampus: mechanism for tonic inhibition. Brain Res. 1980; 200:195–200. [PubMed: 7417806]

Alle H, Geiger JR. Combined analog and action potential coding in hippocampal mossy fibers. Science. 2006; 311:1290–1293. [PubMed: 16513983]

Arima J, Kubo C, Ishibashi H, Akaike N. alpha2-Adrenoceptor-mediated potassium currents in acutely dissociated rat locus coeruleus neurones. J Physiol. 1998; 508(Pt 1):57–66. [PubMed: 9490817]

Bean BP. Neurotransmitter inhibition of neuronal calcium currents by changes in channel voltage dependence. Nature. 1989; 340:153–156. [PubMed: 2567963]

Bell CC, Han V, Sawtell NB. Cerebellum-like structures and their implications for cerebellar function. Annu Rev Neurosci. 2008; 31:1–24. [PubMed: 18275284]

Bender KJ, Ford CP, Trussell LO. Dopaminergic modulation of axon initial segment calcium channels regulates action potential initiation. Neuron. 2010; 68:500–511. [PubMed: 21040850]

Berridge CW, Waterhouse BD. The locus coeruleus-noradrenergic system: modulation of behavioral state and state-dependent cognitive processes. Brain Res Brain Res Rev. 2003; 42:33–84. [PubMed: 12668290]

Boudreau CE, Ferster D. Short-term depression in thalamocortical synapses of cat primary visual cortex. J Neurosci. 2005; 25:7179–7190. [PubMed: 16079400]

Cafaro J, Rieke F. Noise correlations improve response fidelity and stimulus encoding. Nature. 2010; 468:964–967. [PubMed: 21131948]

Carr DB, Andrews GD, Glen WB, Lavin A. alpha2-Noradrenergic receptors activation enhances excitability and synaptic integration in rat prefrontal cortex pyramidal neurons via inhibition of HCN currents. J Physiol. 2007; 584:437–450. [PubMed: 17702809]

Castro-Alamancos MA, Oldford E. Cortical sensory suppression during arousal is due to the activity-dependent depression of thalamocortical synapses. J Physiol. 2002; 541:319–331. [PubMed: 12015438]

Davis KA, Miller RL, Young ED. Effects of somatosensory and parallel-fiber stimulation on neurons in dorsal cochlear nucleus. J Neurophysiol. 1996; 76:3012–3024. [PubMed: 8930251]

Davis KA, Young ED. Granule cell activation of complex-spiking neurons in dorsal cochlear nucleus. J Neurosci. 1997; 17:6798–6806. [PubMed: 9254690]

Dodt HU, Eder M, Schierloh A, Zieglgansberger W. Infrared-guided laser stimulation of neurons in brain slices. Sci STKE. 2002; 2002:pl2. [PubMed: 11854538]

Dunlap K, Fischbach GD. Neurotransmitters decrease the calcium conductance activated by depolarization of embryonic chick sensory neurones. J Physiol. 1981; 317:519–535. [PubMed: 6118434]

Freedman R, Hoffer BJ, Puro D, Woodward DJ. Noradrenaline modulation of the responses of the cerebellar Purkinje cell to afferent synaptic activity. Br J Pharmacol. 1976; 57:603–605. [PubMed: 963346]

Frerking M, Ohliger-Frerking P. Functional consequences of presynaptic inhibition during behaviorally relevant activity. J Neurophysiol. 2006; 96:2139–2143. [PubMed: 16775209]

Fujino K, Oertel D. Bidirectional synaptic plasticity in the cerebellum-like mammalian dorsal cochlear nucleus. Proc Natl Acad Sci U S A. 2003; 100:265–270. [PubMed: 12486245]

Gentet LJ, Avermann M, Matyas F, Staiger JF, Petersen CC. Membrane potential dynamics of GABAergic neurons in the barrel cortex of behaving mice. Neuron. 2010; 65:422–435. [PubMed: 20159454]

Golding NL, Oertel D. Physiological identification of the targets of cartwheel cells in the dorsal cochlear nucleus. J Neurophysiol. 1997; 78:248–260. [PubMed: 9242277]

Groh A, de Kock CP, Wimmer VC, Sakmann B, Kuner T. Driver or coincidence detector: modal switch of a corticothalamic giant synapse controlled by spontaneous activity and short-term depression. J Neurosci. 2008; 28:9652–9663. [PubMed: 18815251]

Hermann J, Pecka M, von Gersdorff H, Grothe B, Klug A. Synaptic transmission at the calyx of Held under in vivo like activity levels. J Neurophysiol. 2007; 98:807–820. [PubMed: 17507501]

Hirata A, Aguilar J, Castro-Alamancos MA. Noradrenergic activation amplifies bottom-up and top-down signal-to-noise ratios in sensory thalamus. J Neurosci. 2006; 26:4426–4436. [PubMed: 16624962]

Hirono M, Obata K. Alpha-adrenoceptive dual modulation of inhibitory GABAergic inputs to Purkinje cells in the mouse cerebellum. J Neurophysiol. 2006; 95:700–708. [PubMed: 16251261]

Hurley LM, Devilbiss DM, Waterhouse BD. A matter of focus: monoaminergic modulation of stimulus coding in mammalian sensory networks. Curr Opin Neurobiol. 2004; 14:488–495. [PubMed: 15321070]

Jones BE, Friedman L. Atlas of catecholamine perikarya, varicosities and pathways in the brainstem of the cat. J Comp Neurol. 1983; 215:382–396. [PubMed: 6863591]

Kim Y, Trussell LO. Ion channels generating complex spikes in cartwheel cells of the dorsal cochlear nucleus. J Neurophysiol. 2007; 97:1705–1725. [PubMed: 17289937]

Klausberger T, Magill PJ, Marton LF, Roberts JD, Cobden PM, Buzsaki G, Somogyi P. Brain-state- and cell-type-specific firing of hippocampal interneurons in vivo. Nature. 2003; 421:844–848. [PubMed: 12594513]

Klepper A, Herbert H. Distribution and origin of noradrenergic and serotonergic fibers in the cochlear nucleus and inferior colliculus of the rat. Brain Res. 1991; 557:190–201. [PubMed: 1747753]

Kondo S, Marty A. Protein kinase A-mediated enhancement of miniature IPSC frequency by noradrenaline in rat cerebellar stellate cells. J Physiol. 1997; 498(Pt 1):165–176. [PubMed: 9023776]

Kossl M, Vater M. Noradrenaline enhances temporal auditory contrast and neuronal timing precision in the cochlear nucleus of the mustached bat. J Neurosci. 1989; 9:4169–4178. [PubMed: 2574231]

Kossl M, Vater M, Schweizer H. Distribution of catecholamine fibers in the cochlear nucleus of horseshoe bats and mustache bats. J Comp Neurol. 1988; 269:523–534. [PubMed: 3372726]

Kreitzer AC, Carter AG, Regehr WG. Inhibition of interneuron firing extends the spread of endocannabinoid signaling in the cerebellum. Neuron. 2002; 34:787–796. [PubMed: 12062024]

Kromer LF, Moore RY. Cochlear nucleus innervation by central norepinephrine neurons in the rat. Brain Res. 1976; 118:531–537. [PubMed: 1009442]

Leao RM, Von Gersdorff H. Noradrenaline increases high-frequency firing at the calyx of held synapse during development by inhibiting glutamate release. J Neurophysiol. 2002; 87:2297–2306. [PubMed: 11976369]

Li Y, van den Pol AN. Direct and indirect inhibition by catecholamines of hypocretin/orexin neurons. J Neurosci. 2005; 25:173–183. [PubMed: 15634779]

Lorente de No, R. The Primary Acoustic Nuclei. New York: Raven Press; 1981.

Mancilla JG, Manis PB. Two distinct types of inhibition mediated by cartwheel cells in the dorsal cochlear nucleus. J Neurophysiol. 2009; 102:1287–1295. [PubMed: 19474167]

Manis PB, Spirou GA, Wright DD, Paydar S, Ryugo DK. Physiology and morphology of complex spiking neurons in the guinea pig dorsal cochlear nucleus. J Comp Neurol. 1994; 348:261–276. [PubMed: 7814691]

May BJ. Role of the dorsal cochlear nucleus in the sound localization behavior of cats. Hear Res. 2000; 148:74–87. [PubMed: 10978826]

Mitchell SJ, Silver RA. Shunting inhibition modulates neuronal gain during synaptic excitation. Neuron. 2003; 38:433–445. [PubMed: 12741990]

Mittmann W, Koch U, Hausser M. Feed-forward inhibition shapes the spike output of cerebellar Purkinje cells. J Physiol. 2005; 563:369–378. [PubMed: 15613376]

Oertel D, Young ED. What's a cerebellar circuit doing in the auditory system? Trends Neurosci. 2004; 27:104–110. [PubMed: 15102490]

Oliva AA Jr, Jiang M, Lam T, Smith KL, Swann JW. Novel hippocampal interneuronal subtypes identified using transgenic mice that express green fluorescent protein in GABAergic interneurons. J Neurosci. 2000; 20:3354–3368. [PubMed: 10777798]

Parra P, Gulyas AI, Miles R. How many subtypes of inhibitory cells in the hippocampus? Neuron. 1998; 20:983–993. [PubMed: 9620702]

Portfors CV, Roberts PD. Temporal and frequency characteristics of cartwheel cells in the dorsal cochlear nucleus of the awake mouse. J Neurophysiol. 2007; 98:744–756. [PubMed: 17581852]

Pouille F, Scanziani M. Enforcement of temporal fidelity in pyramidal cells by somatic feed-forward inhibition. Science. 2001; 293:1159–1163. [PubMed: 11498596]

Roberts MT, Bender KJ, Trussell LO. Fidelity of complex spike-mediated synaptic transmission between inhibitory interneurons. J Neurosci. 2008; 28:9440–9450. [PubMed: 18799676]

Roberts MT, Trussell LO. Molecular layer inhibitory interneurons provide feedforward and lateral inhibition in the dorsal cochlear nucleus. J Neurophysiol. 2010; 104:2462–2473. [PubMed: 20719922]

Ruigrok TJ, Hensbroek RA, Simpson JI. Spontaneous activity signatures of morphologically identified interneurons in the vestibulocerebellum. J Neurosci. 2011; 31:712–724. [PubMed: 21228180]

Salin PA, Prince DA. Spontaneous GABAA receptor-mediated inhibitory currents in adult rat somatosensory cortex. J Neurophysiol. 1996; 75:1573–1588. [PubMed: 8727397]

Shore SE. Multisensory integration in the dorsal cochlear nucleus: unit responses to acoustic and trigeminal ganglion stimulation. Eur J Neurosci. 2005; 21:3334–3348. [PubMed: 16026471]

Shu Y, Hasenstaub A, Duque A, Yu Y, McCormick DA. Modulation of intracortical synaptic potentials by presynaptic somatic membrane potential. Nature. 2006; 441:761–765. [PubMed: 16625207]

Solis MM, Perkel DJ. Noradrenergic modulation of activity in a vocal control nucleus in vitro. J Neurophysiol. 2006; 95:2265–2276. [PubMed: 16371453]

Sutherland DP, Glendenning KK, Masterton RB. Role of acoustic striae in hearing: discrimination of sound-source elevation. Hear Res. 1998; 120:86–108. [PubMed: 9667434]

Swadlow HA. Thalamocortical control of feed-forward inhibition in awake somatosensory 'barrel' cortex. Philos Trans R Soc Lond B Biol Sci. 2002; 357:1717–1727. [PubMed: 12626006]

Telgkamp P, Raman IM. Depression of inhibitory synaptic transmission between Purkinje cells and neurons of the cerebellar nuclei. J Neurosci. 2002; 22:8447–8457. [PubMed: 12351719]

Thompson AM. Pontine sources of norepinephrine in the cat cochlear nucleus. J Comp Neurol. 2003; 457:374–383. [PubMed: 12561077]

Tzounopoulos T, Kim Y, Oertel D, Trussell LO. Cell-specific, spike timing-dependent plasticities in the dorsal cochlear nucleus. Nat Neurosci. 2004; 7:719–725. [PubMed: 15208632]

Tzounopoulos T, Rubio ME, Keen JE, Trussell LO. Coactivation of pre- and postsynaptic signaling mechanisms determines cell-specific spike-timing-dependent plasticity. Neuron. 2007; 54:291–301. [PubMed: 17442249]

Vincent P, Marty A. Fluctuations of inhibitory postsynaptic currents in Purkinje cells from rat cerebellar slices. J Physiol. 1996; 494(Pt 1):183–199. [PubMed: 8814615]

Waterhouse BD, Woodward DJ. Interaction of norepinephrine with cerebrocortical activity evoked by stimulation of somatosensory afferent pathways in the rat. Exp Neurol. 1980; 67:11–34. [PubMed: 7349980]

Williams JT, Henderson G, North RA. Characterization of alpha 2-adrenoceptors which increase potassium conductance in rat locus coeruleus neurones. Neuroscience. 1985; 14:95–101. [PubMed: 2579354]

Williams JT, North RA. Catecholamine inhibition of calcium action potentials in rat locus coeruleus neurones. Neuroscience. 1985; 14:103–109. [PubMed: 2579349]

Zeilhofer HU, Studler B, Arabadzisz D, Schweizer C, Ahmadi S, Layh B, Bosl MR, Fritschy JM. Glycinergic neurons expressing enhanced green fluorescent protein in bacterial artificial chromosome transgenic mice. J Comp Neurol. 2005; 482:123–141. [PubMed: 15611994]

Zhang S, Oertel D. Cartwheel and superficial stellate cells of the dorsal cochlear nucleus of mice: intracellular recordings in slices. J Neurophysiol. 1993; 69:1384–1397. [PubMed: 8389821]

Zhang S, Oertel D. Neuronal circuits associated with the output of the dorsal cochlear nucleus through fusiform cells. J Neurophysiol. 1994; 71:914–930. [PubMed: 8201432]

Zhao Y, Rubio ME, Tzounopoulos T. Distinct functional and anatomical architecture of the endocannabinoid system in the auditory brainstem. J Neurophysiol. 2009; 101:2434–2446. [PubMed: 19279154]

Zhao Y, Tzounopoulos T. Physiological Activation of Cholinergic Inputs Controls Associative Synaptic Plasticity via Modulation of Endocannabinoid Signaling. J Neurosci. 2011; 31:3158–3168. [PubMed: 21368027]

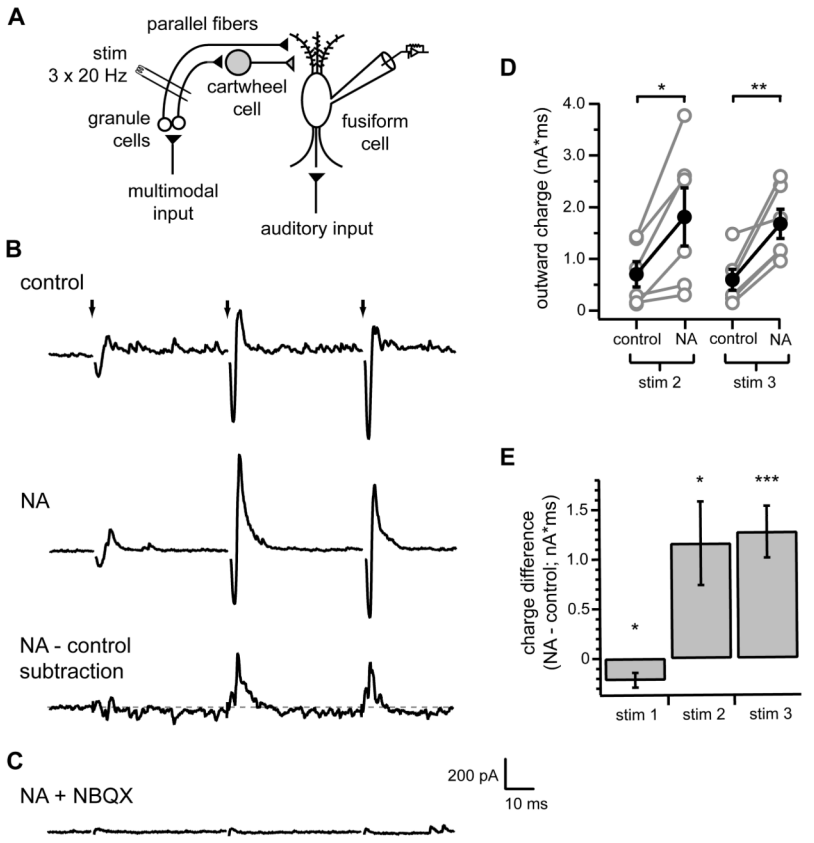

Figure 1. NA enhances parallel fiber-evoked feed-forward inhibition of DCN fusiform cells

(A) Simplified DCN circuit diagram. Black and gray triangles represent glutamatergic and glycinergic/GABAergic synaptic terminals, respectively. Recording and stimulus (stim) electrodes illustrate experimental configuration for (B–G).

(B) Example responses to identical parallel fiber stimulation (3 stimuli at 20 Hz, arrows) recorded from a fusiform cell in control conditions (top) or in 10 μM NA (middle). Bottom trace shows difference current calculated from subtraction of response in control from response in NA. Gray dotted line is zero current level. (C) NBQX eliminated both inward and outward components of evoked responses, confirming disynaptic nature of outward currents. Same cell as in (B).(D) Summary of total charge of outward components (see Methods) of second and third responses in control and NA. Gray circles are data from individual cells. Filled black circles with error bars represent mean±SEM of outward charge measurements. NA significantly increased outward charge for both stimulus 2 (*$p<0.05$) and 3 (**$p<0.01$), n=6.

(E) Summary of mean total charge measurements after each stimulus (20 ms window) determined from subtraction currents as shown in (E). Charge difference significantly different from 0 pA*ms for all stimuli (stim1 *$p<0.05$, stim2 *$p<0.05$, stim3 ***$p<0.005$), one sample t-tests, n=6.

In (B–C), current traces are averages of 20 sweeps. Stimulus artifacts were removed from (B, top and middle, C) for clarity. Scale bars apply to all current traces.

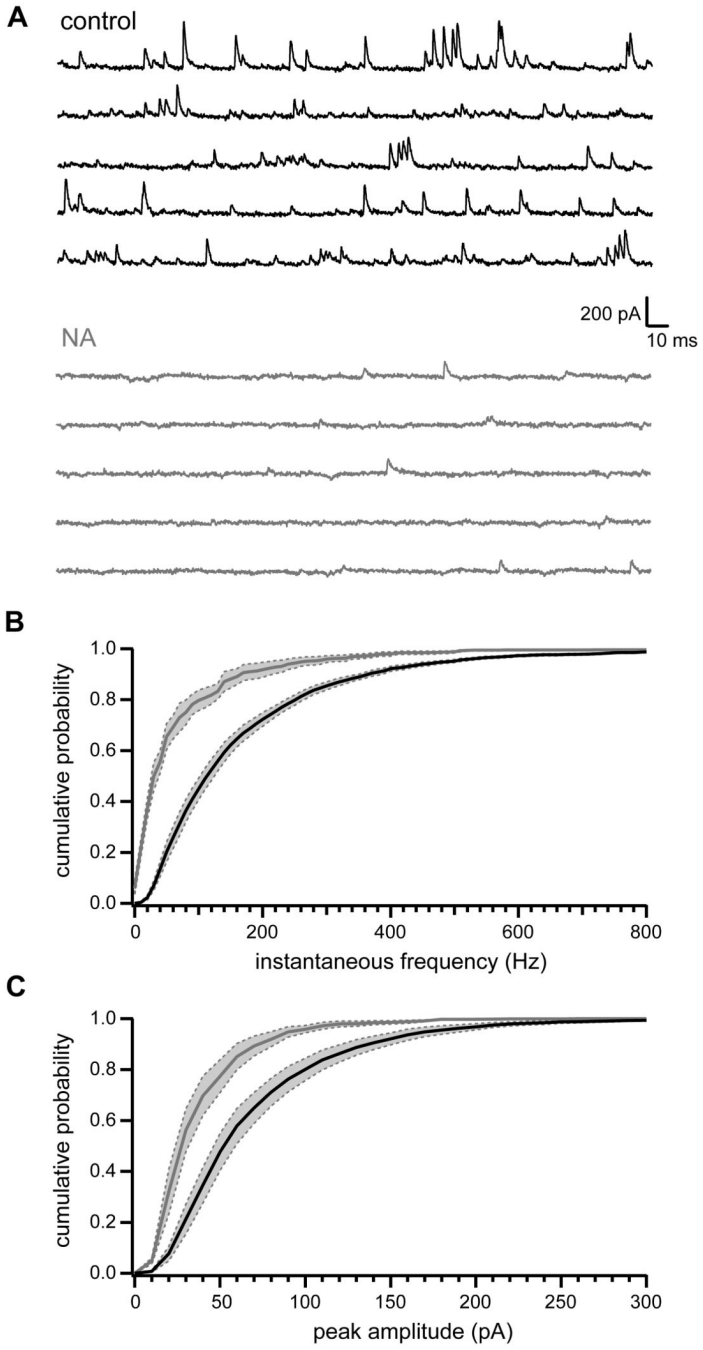

Figure 2. NA reduces spontaneous IPSCs recorded in fusiform cells

(A) Current traces recorded from an example fusiform cell in control conditions (black, top) and 10 μM NA (gray, bottom). Traces are from a different cell than that shown in Figure 1.

(B) Cumulative probability histogram of inter-event instantaneous frequencies for fusiform cell sIPSCs. Black line and gray line are mean sIPSC instantaneous frequencies in control and NA, respectively, n=6 cells. Dotted gray lines bounding shaded gray regions show SEM. Distributions are significantly different, $p<0.0001$, Kolmogorov-Smirnov test.

(C) Same as (B) but for sIPSC peak amplitude measurements. Data in (B–C) from same cells as in Figure 1. Distributions are significantly different, $p<0.0001$, Kolmogorov-Smirnov test.

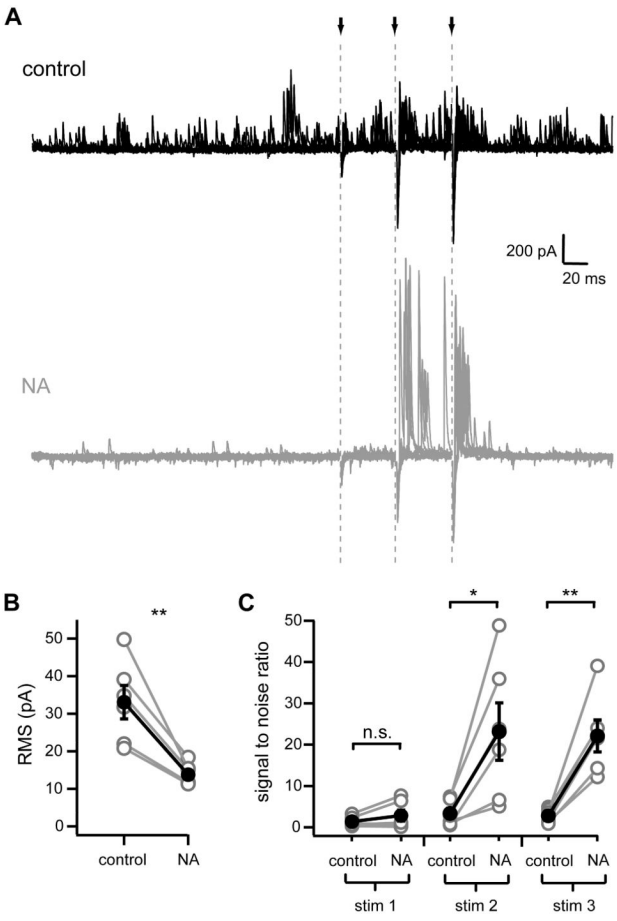

Figure 3. NA enhances signal-to-noise of parallel fiber-evoked inhibition

(A) Overlays of ten current traces recorded from a fusiform cell in control (black, top) and in 10 μM NA (gray, bottom). Arrows and gray dotted lines show times of parallel fiber stimulation. Same cell as in Figure 2A. Stimulus artifacts were removed for clarity.

(B) RMS measurements in control and NA. Gray circles are data from individual cells. Filled black circles with error bars are mean±SEM. **p< 0.005, n=6.

(C) Signal-to-noise ratios calculated by dividing peak amplitude of outward currents following each stimulus by RMS measurements. *p< 0.02, **p<0.005, n=6. Data from same cells shown in Figures 1, 2.

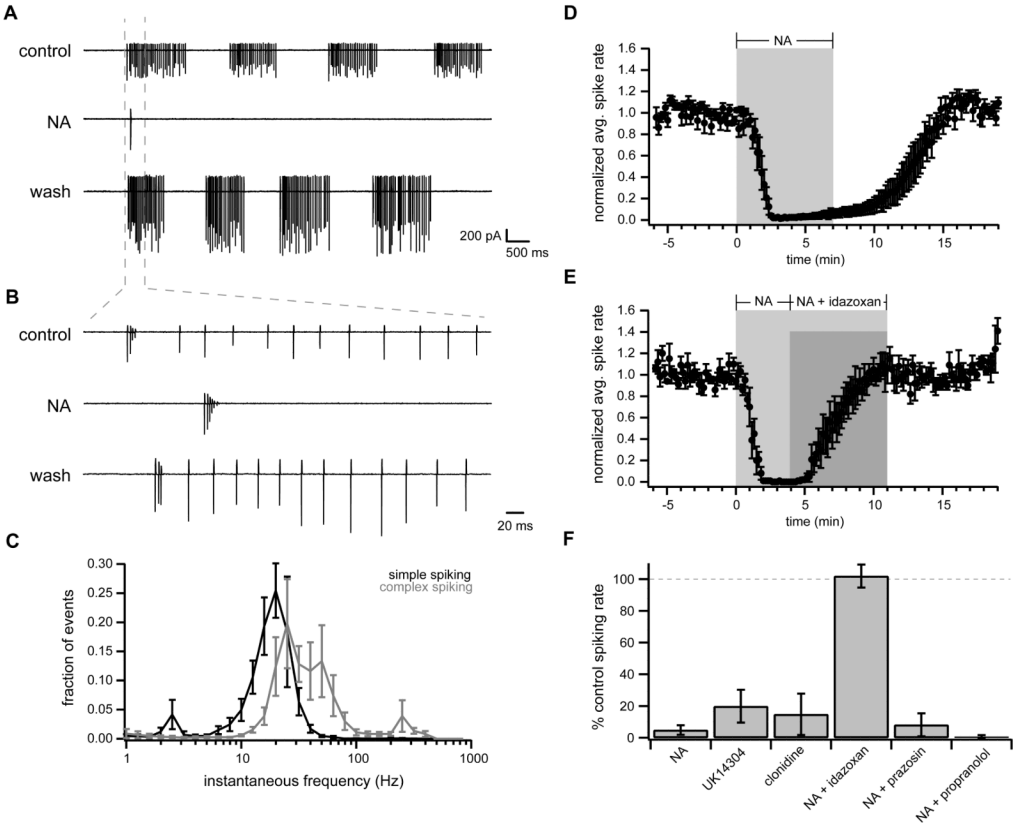

Figure 4. NA eliminates cartwheel cell spontaneous spiking via α_2 adrenergic receptors

(A) Example loose cell-attached recording from spontaneously spiking cartwheel in control (top), NA (10 μM; middle), and after washout of NA (bottom).

(B) Region of traces from (A) within gray dotted lines with expanded time base. Note presence of both complex and simple spikes in this cell.

(C) Normalized histogram of instantaneous spike frequencies from cartwheels with primarily simple spikes (simple spiking, black; defined as cells with <1% of interspike intervals >100 Hz, n= 5) and those with both complex and simple spikes (complex spiking, gray; >1% interspike intervals >100 Hz, n=6).

(D) Time course of spontaneously cartwheel cell spike rate normalized to mean baseline rate. NA (10 μM) was bath applied during time demarcated by gray box. n=6.

(E) Time course of spontaneously spiking cartwheel cell responses to NA (10 μM; gray box) followed by co-application of NA with idazoxan (1 μM; dark gray box). n=5 cells. Filled circles and error bars in (D–E) are mean ± SEM.

(F) Summarized data (mean ± SEM) for spontaneously spiking cartwheel responses with respect to baseline spike rate. NA data is from cells shown in (D). NA + idazoxan data is from cells shown in (E). UK14304: 1 μM, n=8; clonidine: 5 μM, n=4; prazosin: 0.1 μM, n=4; propranolol: 20 μM, n=6. All groups are not significantly different from NA group with the exception of NA + idazoxan ($p<0.0002$), which is not significantly different from 100% of control spike rate ($p=0.80$, one sample t-test).

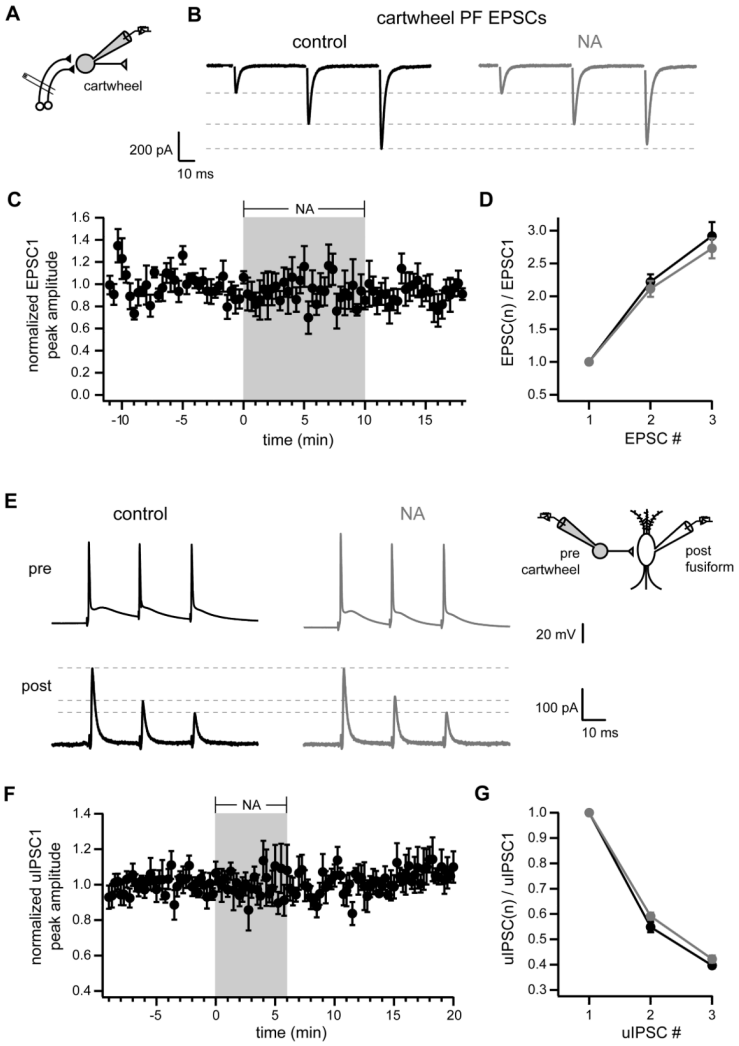

Figure 5. No direct effect of NA on parallel fiber or cartwheel synapses

(A) Experimental configuration for (B–D)

(B) Average current traces from example cartwheel cell in control (black, left) and 10 μM NA (gray, right). Stimulus artifacts were removed for clarity.

(C) Time course of peak amplitudes of first PF EPSC normalized to mean baseline peak amplitude. NA (10 μM) bath applied during period outlined by gray box.

(D) Ratios of EPSC peak amplitudes with respect to first EPSC. Black is control data, gray shows responses in NA. (C–D) n=6. No significant differences between control and NA.

(E) Example simultaneous recordings from synaptically connected cartwheel (top, single voltage traces) and fusiform (bottom, averaged current traces). Brief, suprathreshold current injections were applied to presynaptic cartwheel to elicit train of three simple spikes at 50 Hz. Black traces (left) recorded in baseline control conditions. Gray traces (right) recorded in 10 μM NA. Inset shows recording configuration.

(F) Time course of first uIPSC peak amplitude normalized to mean baseline uIPSC peak amplitude. 10 μM NA bath applied during gray box.

(G) Ratios of uIPSC peak amplitudes with respect to first uIPSC. Black, control; gray, NA. (F–G) n=6. No significant differences between control and NA.

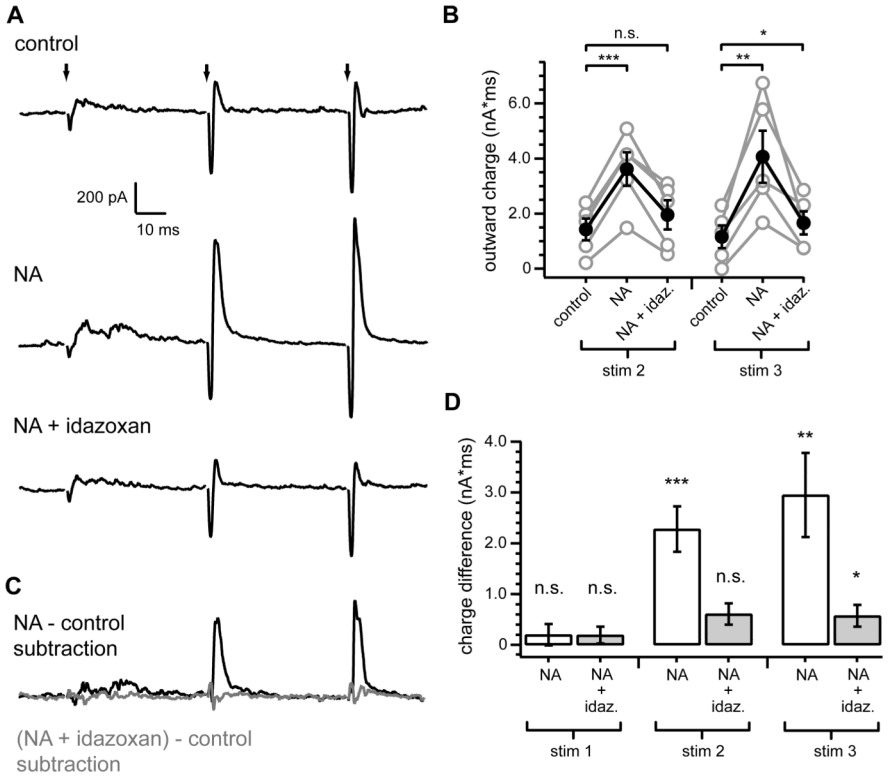

Figure 6. Noradrenergic enhancement of feed-forward inhibition requires α2 adrenergic receptors

(A) Top, example fusiform cell averaged response to train stimuli of parallel fiber inputs (3 stim at 20 Hz) (identical experimental configuration to Figure 1). Middle, response of same cell to identical stimulus, but in NA (10 μM). Bottom, subsequent response of same cell to same stimulus, with co-application of idazoxan (1 μM) and NA). (B) Summary of outward charge measurements for second and third stimuli. Gray circles are data from individual cells. Filled black circles with error bars show mean ± SEM. Outward charge after second stimulus was significantly increased from control in NA (***$p < 0.001$), but not in NA + idazoxan ($p=0.1$). Outward charge after third stimulus was significantly increased from control in NA (**$p<0.01$) and slightly, but significantly, increased in NA + idazoxan (*$p=0.047$), n=5.

(C) Subtraction of response in control (A, top) from response in NA (A, middle) is shown in black. Subtraction of response in control (A, top) from response in NA+ idazoxan (A, bottom) is shown in gray.

(D) Summary of mean total charge measurements after each stimulus (20 ms window) from subtracted currents as shown in E. Charge difference measurements are significantly different from 0 pA*ms for stim2 NA (***$p<0.002$) and stim3 NA (**$p<0.01$) and NA + idazoxan (*$p<0.05$), but not for stim1 NA ($p=0.46$) and NA + idazoxan ($p=0.29$) or stim2 NA + idazoxan ($p=0.053$), one sample t-test, n=5.

Stimulus artifacts in (A) were blanked for clarity. Current traces are averages from 20 consecutive sweeps. Scale bars apply to all current traces.

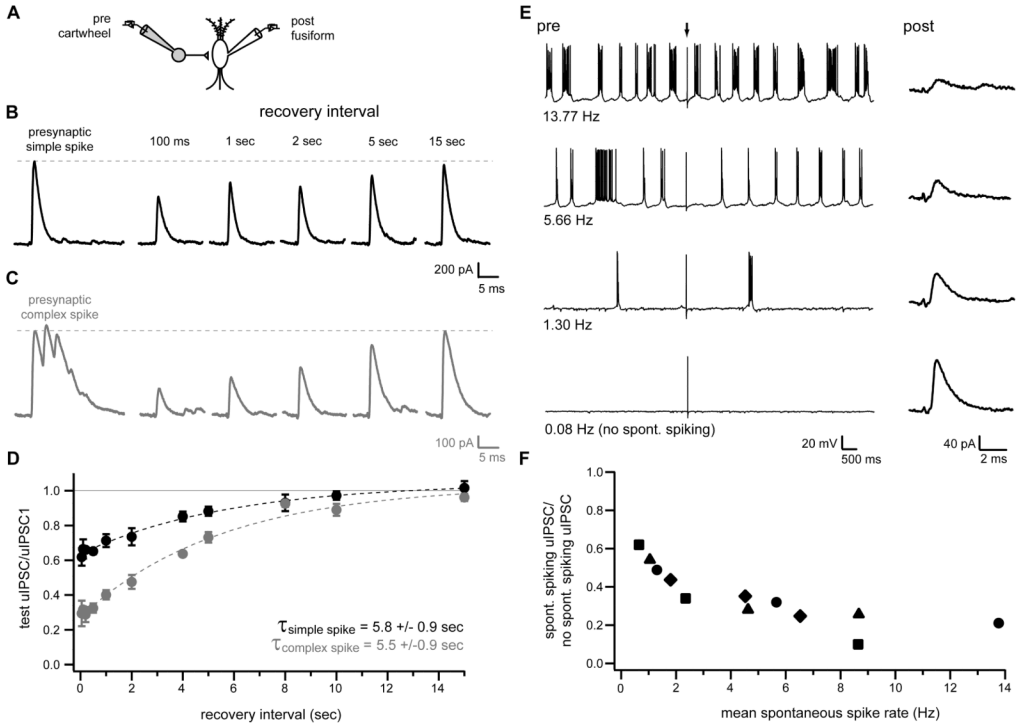

Figure 7. Depression of cartwheel synapses during spontaneous spiking

(A) Recording configuration for (B–F).

(B, C) Postsynaptic fusiform cell responses to simple (B; black) or complex (C; gray) spikes in presynaptic cartwheel cell (leftmost traces) and to subsequent presynaptic simple spikes elicited at various time intervals after the initial simple or complex spikes. Presynaptic spikes were elicited by brief, suprathreshold current injection. Presynaptic cartwheels were either not spontaneously active, or were held below threshold for spontaneous activity by steady bias current injection for the duration of experiments in (B–D). Traces in (B) and (C) are from different pairs and are averages of 8–15 sweeps.

(D) Summary of experiments as in (B) and (C) plotted as ratio of uIPSC peak amplitudes at different recovery intervals with respect to peak amplitude of response to initial simple spike (black circles; n=5 pairs except for 100 ms interval, n=4) or first spikelet of initial complex spike (gray circles; n=5 pairs except for 50 ms, 100 ms, 200 ms and 10 s intervals, n=4). Dotted lines are exponential fits to the data.

(E) Left traces show example voltage records from a presynaptic cartwheel cell held at different mean spontaneous firing rates by steady bias current injection. Arrow indicates time at which brief intracellular current injection was applied to elicit a single simple spike. Right traces show average currents (12–19 sweeps) recorded from postsynaptic fusiform cell in response current injection-triggered simple spikes in presynaptic cartwheels (arrow; 12 seconds between injections) at the different presynaptic spontaneous firing rates.

(F) Summary of experiments as shown in (E). Data for different spontaneous rates plotted as peak uIPSC amplitude with respect to uIPSC peak amplitude without background spontaneous firing (0.08 Hz condition). n=4 pairs (data points with shared symbols are from same pairs).

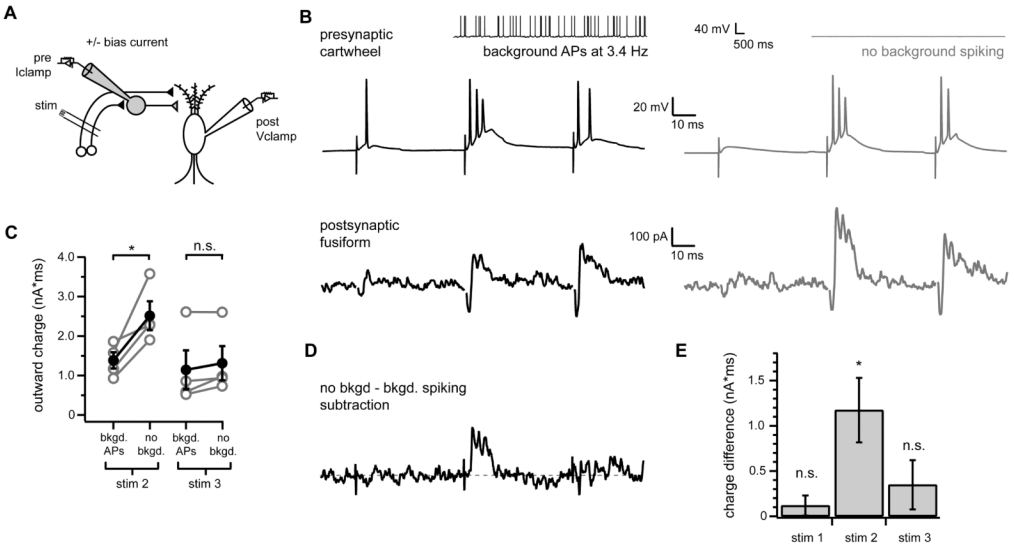

Figure 8. Modulation of cartwheel spontaneous spiking alters feed-forward inhibition of fusiform cells

(A) Experimental configuration.

(B) Example traces from connected cartwheel-fusiform pair in response to train stimulation of parallel fiber inputs to both cells. The presynaptic cartwheel (top traces) was held in current clamp and steady bias current was applied to induce the cell to either spike spontaneously (black traces on left, see inset, mean background firing rate was 3.4 Hz), or to remain silent (gray traces on right) in the absence of parallel fiber stimulation. Bottom traces show average fusiform cell responses to parallel fiber stimulation measured in voltage clamp under either presynaptic firing condition. Note enhancement of outward component of fusiform response to second parallel fiber stimulus without background presynaptic spiking (gray trace) compared to responses during background presynaptic firing (black trace). Stimulus artifacts were removed from fusiform cell current traces for clarity.

(C) Summary of outward charge measurements for second and third stimuli for experiments as shown in A, n=4 pairs. Gray circles show data for individual pairs. Filled black circles with error bars show mean±SEM for all pairs. The outward component of the response to the second parallel fiber stimulus was significantly larger when presynaptic cartwheels were not spiking spontaneously (no bkgd.) compared to when they were induced to fire spontaneously (bkgd APs), *$p < 0.05$.(D) Difference current from subtraction of fusiform current trace shown on left in (B) (presynaptic background APs) from trace shown in (B), right (no background spiking condition).

(E) Summary of mean total charge measurements after each stimulus (20 ms window) between no background and background spiking conditions determined from subtraction currents as shown in (D). Charge difference significantly different from 0 pA*ms for stim2 (*$p<0.05$), but not stim 1 or stim 3 ($p=0.36$, 0.29, respectively), one sample t-test, n=4.